the purple acid phosphatases may employ this unique metal site to catalyze hydrolysis of phosphate esters in a significantly different manner.

Acknowledgment. This work was supported by a grant from the National Science Foundation (DMB-8804931). S.S.D. is grateful for a graduate fellowship from the Amoco Foundation. We are also grateful to Dr. J. D. Lipscomb, A. Orville, and M. Harpel for helpful discussions concerning ^{17}O experiments. The efforts of Dr. R. E. Norman in the preparation of the $Na_2[FeZn(HXTA)(OAc)_2]$ complex are also appreciated.

Registry No. PO_4^{3-}, 14265-44-2; AsO_4^{3-}, 15584-04-0; MoO_4^{2-}, 14259-85-9.

Supplementary Material Available: Lineweaver-Burke plots of uteroferrin inhibition by molybdate (2 pages). Ordering information is given on any current masthead page.

Liquid-Phase ESR, ENDOR, and TRIPLE Resonance of Porphycene Anion Radicals

Jenny Schlüpmann,[†] Martina Huber,[‡] Moshe Toporowicz,[§] Martin Plato,[†] Matthias Köcher,[⊥] Emanuel Vogel,[⊥] Haim Levanon,[§] and Klaus Möbius*,[†]

Contribution from the Institut für Molekülphysik, Freie Universität Berlin, Arnimallee 14, 1000 Berlin 33, West Germany, Institut für Organische Chemie, Freie Universität Berlin, Takustrasse 3, 1000 Berlin 33, West Germany, Department of Physical Chemistry and The Fritz Haber Research Center for Molecular Dynamics, The Hebrew University of Jerusalem, Jerusalem, 91904 Israel, and Institut für Organische Chemie, Universität Köln, Greinstrasse 4, 5000 Köln, West Germany. *Received November 17, 1989*

Abstract: Porphycenes are novel structural isomers of porphyrins. The radical anions of several porphycenes were studied by ESR, ENDOR, and TRIPLE resonance in liquid solution yielding the isotropic hyperfine coupling constants including signs. For the unsubstituted free-base porphycene, the 2,7,12,17-tetra-*n*-propylporphycene, and the 9,10,19,20-tetra-*n*-propylporphycene, the experimental findings are compared with results of all-valence-electrons self-consistent field molecular orbital calculations (RHF-INDO/SP).

Introduction

The porphyrins and metalloporphyrins constitute the essential chromophores in many photochemical and photobiological processes. It is for this and other reasons that the porphycenes (Figure 1), a new class of planar tetrapyrrolic macrocycles, structurally isomeric to the porphyrins, have invited a thorough study of their physical and chemical properties.[1,2]

Investigations on the role porphycenes may play in photophysical and photochemical processes have just started.[3-5] The difference in molecular structure and symmetry between porphyrins and porphycenes manifests itself clearly in the spectroscopic properties of these compounds as already shown by studies on photoexcited singlet and triplet states.[3-5] A comparison of porphycenes and porphyrins, especially from the viewpoint of electronic structure and photochemical reactivity, must also include an inspection of the doublet-state radical ions of porphycenes. In a short communication, first ESR and multiple electron-nuclear resonance characterizations of the free-base porphycene anion radical have been reported.[6a] From independent investigations, electrochemical, ESR, ENDOR, and EXAFS characterizations of a nickel(II) porphycene anion radical have been reported very recently.[6b,c]

In the present publication we report in more detail on ESR, electron-nuclear double resonance (ENDOR), and electron-nuclear-nuclear triple resonance (TRIPLE) measurements of isotropic interaction parameters such as *g*-factors and ^1H and ^{14}N hyperfine coupling constants (hfc's) of the anion radicals of the following porphycenes (see Figure 1): **1**, unsubstituted free-base porphycene (H_2PC1); **2**, 2,7,12,17-tetra-*n*-propylporphycene (H_2PC2); **3**, 9,10,19,20-tetra-*n*-propylporphycene (H_2PC3); **4**, unsubstituted zinc porphycene (ZnPC1); **5**, 2,7,12,17-tetra-*n*-propylnickel porphycene (NiPC2); **6**, 2,7,12,17-tetra-*n*-propylpalladium porphycene (PdPC2); and **7**, 2,7,12,17-tetra-*n*-propylplatinum porphycene (PtPC2). The spectroscopic results for $H_2PC1^{\bullet-}$, $H_2PC2^{\bullet-}$, and $H_2PC3^{\bullet-}$ are compared with spin density distributions obtained from all-valence-electrons self-consistent field molecular orbital (SCF MO) calculations of the type RHF-INDO/SP.[7]

Experimental Section

The porphycenes were reduced chemically with sodium metal under high-vacuum conditions.[8] Tetrahydrofuran (THF) dried over a Na/K alloy was used as a solvent. The porphycene concentration was about 5×10^{-4} M. The radicals were stable over at least several weeks when stored at −27 °C. The anion radicals of H_2PC1 were also generated by potentiostatically controlled electrolysis in THF using tetra-*n*-butyl-

[†] Institut für Molekülphysik, Freie Universität Berlin.
[‡] Institut für Organische Chemie, Freie Universität Berlin. Present address: University of California San Diego, Department of Physics, La Jolla, CA 92093.
[§] The Hebrew University of Jerusalem.
[⊥] Universität Köln.

(1) (a) Vogel, E.; Köcher, M.; Schmickler, H.; Lex, J. *Angew. Chem.* **1986**, *98*, 262; *Angew. Chem., Int. Ed. Engl.* **1986**, *25*, 257. (b) Vogel, E.; Köcher, M.; Lex, J.; Ermer, O. *Isr. J. Chem.* **1989**, *29*, 257.
(2) Köcher, M. Ph.D. Thesis, Universität Köln, West Germany, 1988.
(3) Ofir, H.; Regev, A.; Levanon, H.; Vogel, E.; Köcher, M.; Balci, M. *J. Phys. Chem.* **1987**, *91*, 2686.
(4) Levanon, H.; Toporowicz, M.; Ofir, H.; Fessenden, R. W.; Das, P. K.; Vogel, E.; Köcher, M.; Pramod, K. *J. Phys. Chem.* **1988**, *92*, 2429.
(5) Toporowicz, M.; Ofir, H.; Levanon, H.; Vogel, E.; Köcher, M.; Pramod, K.; Fessenden, R. W. *Photochem. Photobiol.* **1989**, *50*, 37.
(6) (a) Schlüpmann, J.; Huber, M.; Toporowicz, M.; Köcher, M.; Vogel, E.; Levanon, H.; Möbius, K. *J. Am. Chem. Soc.* **1988**, *110*, 8566. (b) Renner, M. W.; Forman, A.; Wu, W.; Chang, C. K.; Fajer, J. *J. Am. Chem. Soc.* **1989**, *111*, 8618. (c) Furenlid, L. R.; Renner, M. W.; Smith, K. M.; Fajer, J. *J. Am. Chem. Soc.* **1990**, *112*, 1634.
(7) Plato, M.; Tränkle, E.; Lubitz, W.; Lendzian, F.; Möbius, K. *Chem. Phys.* **1986**, *107*, 185.
(8) Paul, D. E.; Lipkin, D.; Weissman, S. I. *J. Am. Chem. Soc.* **1956**, *78*, 116.

0002-7863/90/1512-6463$02.50/0

Table I. Hyperfine Coupling Constants of Porphycene Anion Radicals

		hfc (MHz)							
		$H_2PC1^{\bullet-}$			$H_2PC2^{\bullet-}$	$H_2PC3^{\bullet-}$	$ZnPC1^{\bullet-}$	$NiPC2^{\bullet-}$	$PdPC2^{\bullet-}$
		sodium reduction[a]	electrolysis[a]	simulation and least-squares fit[b]	sodium reduction[a]	sodium reduction[a]	sodium reduction[a]	sodium reduction[a]	sodium reduction[a]
H:	a_1	+0.53	+0.51	0.50	+0.48	+0.42			
	a_2	-2.65	-2.68	2.63	-2.53		-2.35	-2.45	-2.40
	a_3	-4.10	-4.10	4.04		-3.82	-4.62		
	a_4	-5.05	-5.03	5.07	-4.41	-5.00	-4.79	-4.04	-3.81
	a_5				+2.95			+3.52	+3.55
	a_6					+0.10			
	a_7					+1.68			
N:	a_N	-2.00	-1.99	2.05	-1.98	-1.95	-1.90	-1.98	-2.10

[a] See caption of Figure 2 for experimental conditions. Experimental error for hfc's: ±0.03 MHz. [b] Component Lorentz line of 43-mG width; number of iterations 1000. [c] The hfc's of $NiPC2^{\bullet-}$ determined by Renner et al.[6b] are 2.49, 3.95, 3.67, and 1.85 MHz.

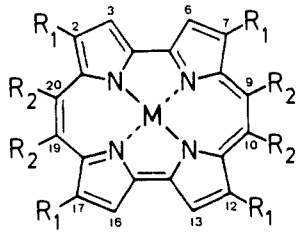

Figure 1. Porphycenes with D_{2h} symmetry as observed on the NMR and ESR time scales. H_2PC1 (parent compound): M = 2 H, $R_1 = R_2 = H$. H_2PC2: M = 2 H, $R_1 = C_3H_7$, $R_2 = H$. H_2PC3: M = 2 H, $R_1 = H$, $R_2 = C_3H_7$. ZnPC1: M = Zn, $R_1 = R_2 = H$. NiPC2: M = Pd, $R_1 = C_3H_7$, $R_2 = H$. PtPC2: M = Pt, $R_1 = C_3H_7$, $R_2 = H$.

ammonium perchlorate (TBAP) as supporting electrolyte.[9] In this case, the porphycene concentration was 10^{-3} M.

Optical spectra of the neutral and anion radical porphycenes were measured in a 3-mm flat quartz cell with a Cary-219 spectrophotometer. The ENDOR and TRIPLE experiments were performed with a self-built computer-controlled X-band spectrometer.[10,11] For ESR measurements, commercial spectrometers (Bruker ER 200 D and Varian E-12) were used.

Results and Discussion

The electronic spectra of porphycenes are characterized by two absorption bands which, in analogy to porphyrins, are assigned as the Q- and B-bands.[3-5] Upon reduction the changes in the electronic spectra are quite noticeable as was recently reported by Renner et al.[6b] for nickel(II) porphycene. Typically, as a main feature associated with the electronic spectra of the porphycene anion radicals, a relative increase of the B-band/Q-band intensity ratio is observed. Some of the reduced porphycenes (in particular, $PdPC2^{\bullet-}$ and $NiPC2^{\bullet-}$) exhibit new absorption bands which are red-shifted relative to the Q-band absorption peaks (for details, see ref 6b). It should be pointed out that all porphycene solutions in the present ESR study were dilute mixtures of the anion radical containing the neutral species, and no attempt was made to analyze quantitatively the electronic spectra of the anion radicals.

As a representative example for the series of porphycenes in this study, H_2PC1 in THF/TBAP has been selected for cyclic voltammetry measurements to establish whether the reduction steps are reversible one-electron processes. The cyclic voltammogram shows two reversible one-electron reductions. The half-wave potentials corresponding to the mono- and dinegative ions of H_2PC1 occur at -0.75 and -1.10 V (±0.02 V) versus saturated calomel electrode (SCE).[12] This finding is in accordance with the results of a recent independent study of free-base Cu^{II} and Ni^{II} tetrapropylporphycene in CH_2Cl_2/TBAP.[6b,c]

Figure 2, a-g, shows the ESR spectra of the different porphycenes. Their g-values and the microwave power levels necessary to saturate the ESR transitions to the extent of maximum ESR signal amplitude are included in the figure. The ESR spectra show partially resolved hyperfine structure. Unlike the ESR spectra of the anion radicals of free-base porphyrins, which do not exhibit resolved hyperfine structure,[14] the ESR spectra of $H_2PC1^{\bullet-}$ and $H_2PC2^{\bullet-}$ are highly structured. This difference in spectral resolution is in part attributed to the fact that the hfc's of the H_2PC1 and H_2PC2 anions are approximately integer multiples of the smallest hfc, a_1 (see Table I). Consequently, accidental ESR line degeneracy occurs, which drastically reduces the number of lines in the spectrum and thereby enhances spectral resolution for the porphycene anions. For the porphyrin anions, the poor resolution of their ESR spectra can be explained as follows. For free-base porphyrins the observed tautomerization[15] of the (N-H) protons is too slow a process to average the molecular D_{2h} symmetry to an apparent D_{4h} symmetry. On the other hand, in solution this jump process might be fast enough to cause additional line broadening. More probably, however, since the orbital degeneracy of the lowest unoccupied MO (LUMO) of the porphyrin π skeleton[16a] is only weakly removed by the central (N-H) protons (our MO calculations predict the orbital energy splitting to be 0.04 eV ≅ 1.6 kT at room temperature), we expect a mixing of states of different symmetry (having different spin density distributions) by thermal fluctuations or by vibrational-electronic interactions.[16b] For the metalloporphyrin anion radicals, which have unperturbed D_{4h} symmetry and a degenerate LUMO,[16a] a dynamical Jahn-Teller effect is expected to produce considerable additional line broadening.[17] The reduced symmetry of porphycene (D_{2h} instead of D_{4h}) is expected to lift the orbital degeneracy leading to smaller line widths.

The ESR spectrum of $H_2PC3^{\bullet-}$, on the other hand, is considerably less resolved although H_2PC2 and H_2PC3 differ only in the sites of the propyl substituents (see Figure 1). As opposed to $H_2PC1^{\bullet-}$ and $H_2PC2^{\bullet-}$, the hfc's of $H_2PC3^{\bullet-}$ are not all integer multiples of the smallest hfc, a_1 (see Table I). This, however, cannot account for such a large decrease in resolution. As will be seen below, additional protons from the substituents contribute to the smallest hfc's of $H_2PC3^{\bullet-}$, thus leading to severe inhomogeneous line broadening.

The ESR spectrum of $ZnPC1^{\bullet-}$ is again highly resolved for the same reason as given for $H_2PC1^{\bullet-}$ and $H_2PC2^{\bullet-}$. The resolution of the ESR spectra of the 2,7,12,17-tetra-*n*-propyl metal por-

(9) Lubitz, W.; Lendzian, F.; Möbius, K. *Chem. Phys. Lett.* **1981**, *81*, 235; **1981**, *84*, 33.
(10) Möbius, K.; Plato, M.; Lubitz, W. *Phys. Rep.* **1982**, *87*, 171.
(11) Lendzian, F. Ph.D. Thesis, Freie Universität Berlin, West Germany, 1982.
(12) In our cyclic voltammetry measurements we used an Ag/AgCl reference electrode. It was calibrated with the ferrocene redox system whose oxidation potential is known[13] to be +0.35 V versus SCE. The potential of the Ag/AgCl electrode versus SCE was measured to be +0.05 V (±0.02 V) in THF/TBAP.
(13) Meites, L.; Zuman, P. *CRC Handbook Series in Organic Electrochemistry*; CRC Press: Cleveland, Ohio, 1977; Vol. I, p 16.
(14) Peychal-Heiling, F.; Wilson, G. S. *Anal. Chem.* **1971**, *43*, 550. Felton, R. H.; Linschitz, H. *J. Am. Chem. Soc.* **1966**, *88*, 1113.
(15) Wehrle, B.; Limbach, H. H.; Köcher, M.; Ermer, O.; Vogel, E. *Angew. Chem.* **1987**, *99*, 914; *Angew. Chem., Int. Ed. Engl.* **1987**, *26*, 934.
(16) (a) Gouterman, M. *J. Mol. Spectrosc.* **1961**, *6*, 138. (b) Bolton, J. R.; Carrington, A.; Forman, A.; Orgel, L. E. *Mol. Phys.* **1962**, *5*, 43.
(17) Townsend, M. G.; Weissman, S. I. *J. Chem. Phys.* **1960**, *32*, 309. McConnell, H. M.; McLachlan, A. D. *J. Chem. Phys.* **1960**, *34*, 1.

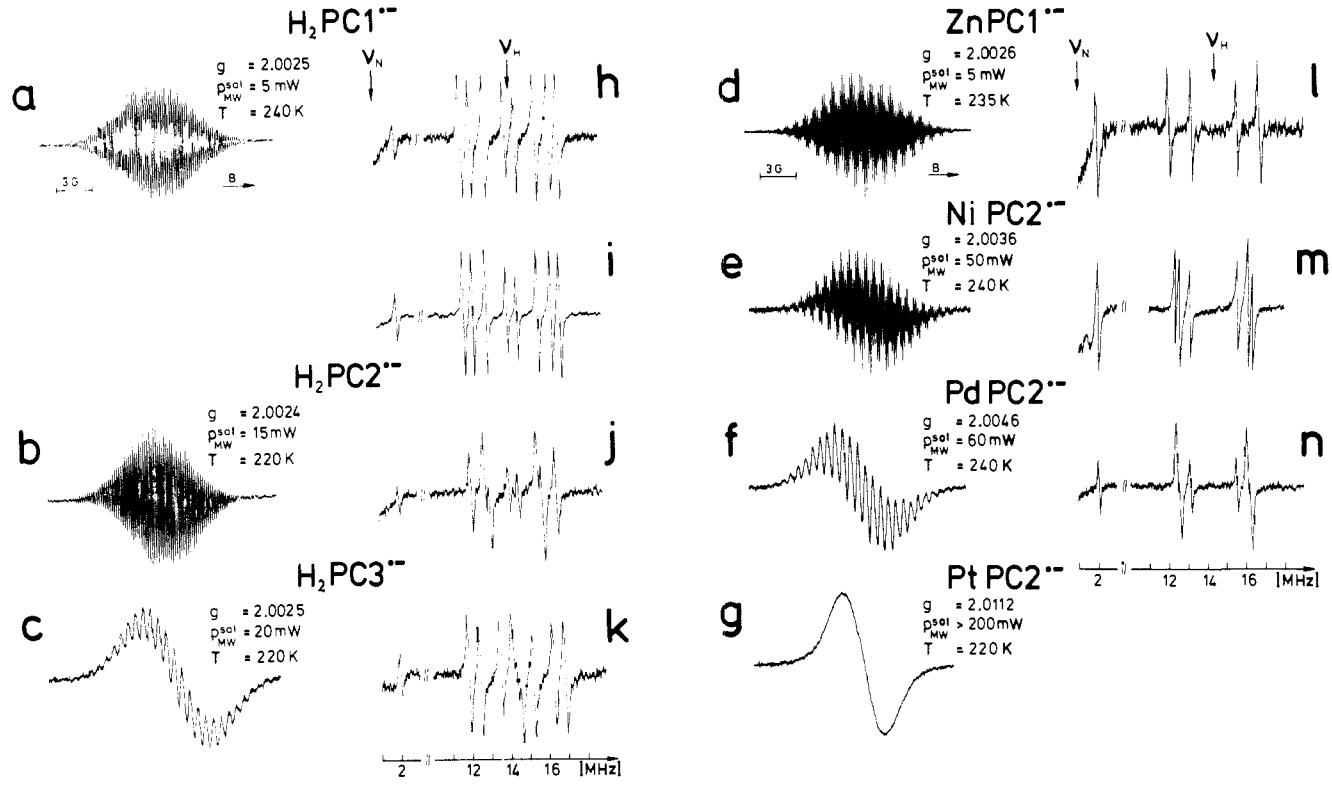

Figure 2. ESR spectra of the porphycene anion radicals in THF. The g-factors are measured with an accuracy of ±0.0001. For $H_2PC2^{\bullet-}$ and $PtPC2^{\bullet-}$ the accuracy is only ±0.0002; for $H_2PC2^{\bullet-}$ the reason is the difficulty of determining the central ESR line, and for $PtPC2^{\bullet-}$ it is the broad inhomogeneous line. P_{mw}^{sat} is the microwave power level at maximum amplitude of the ESR signal. ^{14}N and ^1H ENDOR spectra of the porphycene anion radicals in THF (experimental conditions noted). (h) $H_2PC1^{\bullet-}$ (sodium reduction): For ^1H ENDOR, T = 193 K, mw power P_{mw} = 5 mW, rf power P_{rf} = 75 W, 10-kHz frequency modulation of rf field, fm = ±40 kHz deviation, no Zeeman modulation, time constant τ = 0.4 s, 6 scans. For ^{14}N ENDOR, T = 256 K, P_{mw} = 5 mW, P_{rf} = 150 W, fm = ±50 kHz, 1-kHz Zeeman modulation, τ = 0.4 s, 6 scans. (i) $H_2PC1^{\bullet-}$ (electrolysis): For ^1H ENDOR, T = 193 K, P_{mw} = 5 mW, P_{rf} = 60 W, fm = ±40 kHz, τ = 0.4 s, 5 scans. For ^{14}N ENDOR, T = 193 K, P_{mw} = 5 mW, P_{rf} = 100 W, fm = ±50 kHz, τ = 0.4 s, 4 scans. (j) $H_2PC2^{\bullet-}$: For ^1H ENDOR, T = 210 K, P_{mw} = 15 mW, P_{rf} = 85 W, fm = ±30 kHz, τ = 0.4 s, 8 scans. For ^{14}N ENDOR, T = 210 K, P_{mw} = 15 mW, P_{rf} = 150 W, fm = ±50 kHz, τ = 0.4 s, 10 scans. (k) $H_2PC3^{\bullet-}$: For ^1H ENDOR, T = 219 K, P_{mw} = 20 mW, P_{rf} = 105 W, fm = ±40 kHz, τ = 0.4 s, 6 scans. For ^{14}N ENDOR, T = 219 K, P_{mw} = 20 mW, P_{rf} = 180 W, fm = ±50 kHz, τ = 0.4 s, 12 scans. (l) $ZnPC1^{\bullet-}$: For ^1H ENDOR, T = 193 K, P_{mw} = 5 mW, P_{rf} = 60 W, fm = ±15 kHz, τ = 0.4 s, 8 scans. For ^{14}N ENDOR, T = 246 K, P_{mw} = 5 mW, P_{rf} = 150 W, fm = ±50 kHz, τ = 0.4 s, 6 scans. (m) $NiPC2^{\bullet-}$: For ^1H ENDOR, T = 193 K, P_{mw} = 50 mW, P_{rf} = 50 W, fm = ±20 kHz, τ = 0.4 s, 5 scans. For ^{14}N ENDOR, T = 219 K, P_{mw} = 50 mW, P_{rf} = 200 W, fm = ±50 kHz, τ = 0.4 s, 5 scans. (n) $PdPC2^{\bullet-}$: For ^1H ENDOR, T = 202 K, P_{mw} = 60 mW, P_{rf} = 100 W, fm = ±30 kHz, τ = 0.4 s, 7 scans. For ^{14}N ENDOR, T = 202 K, P_{mw} = 50 mW, P_{rf} = 140 W, fm = ±50 kHz, τ = 0.4 s, 7 scans.

phycene anion radicals degrades with increasing atomic weight of the metal. The increase of ESR line width goes parallel with an increase of the g-factor as well as an increase of the microwave power level necessary to saturate the ESR transition. This behavior originates in the spin–orbit coupling mechanism. Larger spin–orbit coupling infers a larger g-factor[18] and thereby a larger contribution of the spin-rotational interaction to the electronic relaxation.[19-21] This is because the contribution of the spin-rotational interaction to the relaxation rates $1/T_{1e}$ and $1/T_{2e}$ is proportional to the deviation of the g-factor from the free electron value, g_e = 2.0023. As a result, higher microwave power is necessary for saturation and an increase in the component line width is observed in the ESR spectra of radicals in which heavy atoms are participating in the conjugation framework. For these reasons the ESR spectrum of $PtPC2^{\bullet-}$ is a single unresolved inhomogeneously broadened Gaussian line. For ENDOR experiments it is necessary to saturate an ESR transition, and this requires higher microwave power levels as the homogeneous ESR line width gets broader. For $PtPC2^{\bullet-}$ even at temperatures as low as 180 K the saturation condition could not be fulfilled with the available microwave power of up to 200 mW, and, consequently, no ENDOR signal could be detected for this radical.

The ENDOR spectra of the investigated porphycene anion radicals are presented in Figure 2, h–n. For a doublet radical in solution, two ENDOR lines per hfc, a_{iso}, are expected at frequencies

$$\nu_{\pm ENDOR} = |\nu_n \pm a_{iso}/2| \quad (1)$$

where $\nu_n = (g_n\mu_N/h)B$ is the nuclear Larmor frequency.[10]

The proton ENDOR spectrum of $H_2PC1^{\bullet-}$ reveals four pairs of lines symmetrically arranged around ν_H which, at the static magnetic field applied in our X-band experiments, has a value of 14.38 MHz (see Figure 2h). The corresponding ^1H hfc's are listed in Table I, both for chemically and electrolytically generated $H_2PC1^{\bullet-}$. At 2.04 MHz one ^{14}N ENDOR line was detected. Since in our experiment the ^{14}N Larmor frequency is 1.04 MHz, according to eq 1, $^1/_2a(N)$ = 1.00 MHz and the corresponding low-frequency ^{14}N ENDOR line is expected at 0.04 MHz, which is below the frequency range of the spectrometer. The relative signs of the ^1H hfc's and the ^{14}N hfc could be determined by "General TRIPLE" experiments.[10,22] The absolute signs of the hfc's given in Table I are based on the assumption that the largest ^1H hfc of $H_2PC1^{\bullet-}$, $|a_4|$ = 5.05 MHz (±30 kHz), originates from a positive carbon $2p_z$ spin density. Therefore, the adjacent α-proton[23] hfc is negative due to σ–π spin polarization.[24]

(18) Atherton, N. M. *Electron Spin Resonance*; Ellis Horwood: Chichester, 1973; p 206.
(19) Freed, J. H. In *Multiple Electron Resonance Spectroscopy*; Dorio, M. M., Freed, J. M., Eds.; Plenum Press: New York, 1979; p 101.
(20) Plato, M.; Lubitz, W.; Möbius, K. *J. Phys. Chem.* **1981**, *85*, 1202.
(21) Leniart, D. S.; Connor, H. D.; Freed, J. H. *J. Chem. Phys.* **1975**, *63*, 165.
(22) Möbius, K.; Biehl, R. In *Multiple Electron Resonance Spectroscopy*; Dorio, M. M., Freed, J. H., Eds.; Plenum Press: New York, 1979; p 475.

The ESR and ENDOR spectra of chemically and electrolytically generated $H_2PC1^{\bullet-}$ are identical within experimental error (see Figure 2, h and i). No hfc of the sodium counterion in the chemically generated samples could be detected by ENDOR, and the line pattern of the ESR spectrum is the same in both cases. This, together with the results from optical spectroscopy and cyclic voltammetry, confirms the identity of the investigated radical anion, which is only loosely interacting with the sodium counterion.

The ENDOR spectrum of $H_2PC2^{\bullet-}$ (Figure 2j) is similar to the one of $H_2PC1^{\bullet-}$, except that one of the two largest ^1H hfc's is missing and an additional positive hfc appears. In the ENDOR spectrum of $H_2PC3^{\bullet-}$ (Figure 2k), a_2 is missing and two additional positive hfc's appear. The ENDOR spectra of $ZnPC1^{\bullet-}$, $NiPC2^{\bullet-}$, and $PdPC2^{\bullet-}$ (Figure 2, l–n) show only three pairs of proton lines; for $ZnPC1^{\bullet-}$ all hfc's are negative, whereas for $NiPC2^{\bullet-}$ and $PdPC2^{\bullet-}$ the second largest hfc is positive. In all the ENDOR spectra, a single ^{14}N line was detected around 2 MHz. No ENDOR spectrum could be obtained from $PtPC2^{\bullet-}$ for reasons given above.

In order to assign the hfc's to specific positions in the molecule, the ENDOR spectra of the various porphycenes were compared with each other. The small ^1H hfc a_1 is equal for $H_2PC1^{\bullet-}$, $H_2PC2^{\bullet-}$, and $H_2PC3^{\bullet-}$, whereas it is missing for the metalloporphycenes, $ZnPC1^{\bullet-}$, $NiPC2^{\bullet-}$, and $PdPC2^{\bullet-}$. Therefore, a_1 must be attributed to the two (N–H) protons of the free-base porphycenes. Similarly, a_2 is equal for $H_2PC1^{\bullet-}$ and $H_2PC2^{\bullet-}$, whereas it is missing for $H_2PC3^{\bullet-}$. Consequently, a_2 is assigned to the set of four equivalent α-protons at positions 9, 10, 19, and 20, and the two sets of equivalent α-protons at the pyrrole rings must correspond to the ^1H hfc's a_3 and a_4. Experimentally we cannot distinguish which one of these α-proton sets contributes to a_3 and which one to a_4. Such an assignment can be made on the basis of MO calculations for $H_2PC1^{\bullet-}$ (see next section). The largest positive hfc in the spectra of $H_2PC2^{\bullet-}$, $NiPC2^{\bullet-}$, and $PdPC2^{\bullet-}$, a_5, is attributed to the set of eight equivalent β-protons of the propyl substituents at positions 2, 7, 12, and 17. The positive sign stems from hyperconjugation,[25] the mechanism by which $2p_z$ spin density of the carbon skeleton extends into the s-orbitals of the substituents.

In a recent independent ESR and ENDOR investigation of $NiPC2^{\bullet-}$, hfc's of similar magnitude and assignment have been inferred;[6b] the hfc at positions 9, 10, 19, and 20 has been assigned directly by deuterium substitution.

From theoretical considerations,[22] it can be shown that the relative line intensities in a "Special TRIPLE"[10,22] spectrum are proportional to the number of contributing protons, provided the nuclear relaxation rate is smaller than the electronic relaxation rate and the NMR transitions are saturated. It is assumed that these conditions are satisfied in our experiments even at temperatures as low as 180 K for the following reasons. First, we know that for $H_2PC1^{\bullet-}$ two protons contribute to a_1 and four protons to each of the other three hfc's. This is reflected in the Special TRIPLE spectrum of $H_2PC1^{\bullet-}$ (see Figure 3a). Secondly, the aforementioned assignment for $H_2PC2^{\bullet-}$ and the metalloporphycenes is compatible with the relative line intensities of their Special TRIPLE spectra. Figure 3 depicts, for example, the Special TRIPLE spectra of $H_2PC1^{\bullet-}$, $H_2PC2^{\bullet-}$, and $NiPC2^{\bullet-}$.

The ESR spectra of the different porphycene anion radicals were computer simulated with the hfc's obtained from ENDOR; the respective number of equivalent protons was chosen according to the aforementioned assignment. For the highly resolved ESR spectrum of $H_2PC1^{\bullet-}$ the simulation was found to be in very good agreement with the experimental spectrum provided four nitrogens were attributed to the single measured ^{14}N hfc (see Figure 4). A simulation with only two nitrogens contributing to the measured

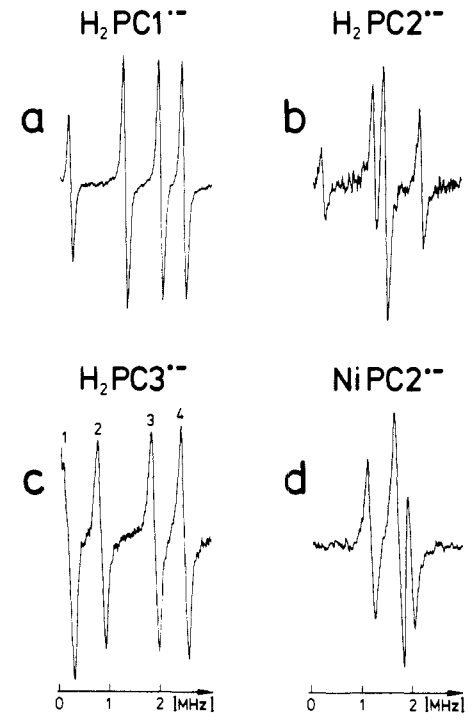

Figure 3. Proton "Special TRIPLE" resonance spectra of $H_2PC1^{\bullet-}$, $H_2PC2^{\bullet-}$, $H_2PC3^{\bullet-}$, and $NiPC2^{\bullet-}$. Experimental conditions: (a) $H_2PC1^{\bullet-}$ (electrolysis): T = 193 K, P_{mw} = 5 mW, P_{rf} = 50 W, fm = ±30 kHz, τ = 0.4 s, 5 scans; (b) $H_2PC2^{\bullet-}$: T = 193 K, P_{mw} = 5 mW, P_{rf} = 65 W, fm = ±20 kHz, τ = 0.4 s, 6 scans; (c) $H_2PC3^{\bullet-}$: T = 219 K, P_{mw} = 20 mW, P_{rf} = 150 W, fm = ±30 kHz, τ = 0.4 s, 6 scans; (d) $NiPC2^{\bullet-}$: T = 219 K, P_{mw} = 50 mW, P_{rf} = 100 W, fm = ±15 kHz, τ = 0.4 s, 4 scans.

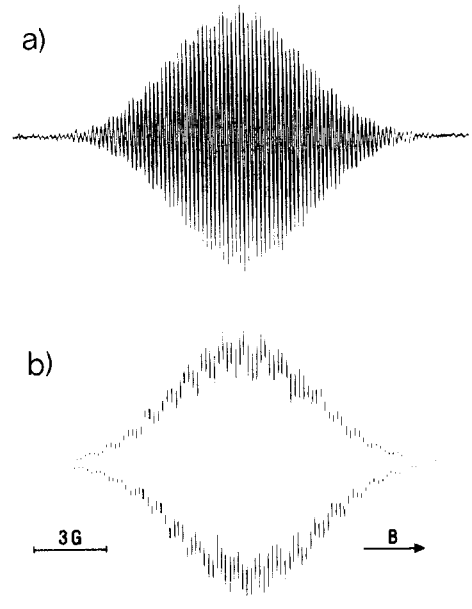

Figure 4. (a) Experimental ESR spectrum of $H_2PC1^{\bullet-}$. (b) Simulation of the ESR spectrum of $H_2PC1^{\bullet-}$. For assignment, see text. A single component line width of 140 kHz was used.

^{14}N hfc does not fit the experimental spectrum. This indicates that, on the ESR time scale and within the experimental resolution, all four nitrogens are equivalent. The equivalence of the four nitrogens is compatible with ^{15}N-CPMAS-NMR experiments[15] which reveal a fast tautomerization of the (N–H) protons even at temperatures as low as 107 K. The ESR spectra of $H_2PC2^{\bullet-}$, $ZnPC1^{\bullet-}$, $NiPC2^{\bullet-}$, and $PdPC2^{\bullet-}$ were also simulated with the assignment described above and under the assumption of all four nitrogens being equivalent. Again, the agreement between simulation and experimental spectra was good. Attempts were also made to simulate the less-resolved ESR spectra with assignments

(23) Throughout this paper, following conventional nomenclature, we call α-, β-, γ-, and δ- protons those protons that are one, two, three, and four bonds away from the π-system, respectively.

(24) Carrington, A.; McLachlan, A. D. *Introduction to Magnetic Resonance*; Harper & Row: New York, 1967; p 83.

(25) Carrington, A.; McLachlan, A. D. *Introduction to Magnetic Resonance*; Harper & Row: New York, 1967; p 109.

differing from the one given above. No convincing agreement with the experimental spectra could be obtained.

The simulated ESR spectrum of $H_2PC1^{\bullet-}$ was also fitted to the experimental ESR spectrum with an iterative least-squares fit program.[26] The resulting slightly modified hfc's are listed in Table I.

The analysis of the ENDOR and Special TRIPLE spectra of $H_2PC3^{\bullet-}$ (Figures 2k and 3c) requires further discussion. By analogy with the spectra of $H_2PC1^{\bullet-}$ and $H_2PC2^{\bullet-}$, a_3 and a_4 are assigned to the two sets of four equivalent α-protons at the pyrrole rings, and a_1 is assigned to the two (N-H) protons. But, compared with the area under the outermost ENDOR lines, the area under the lines corresponding to a_1 is significantly larger for $H_2PC3^{\bullet-}$ than for $H_2PC1^{\bullet-}$ or $H_2PC2^{\bullet-}$ (see Figure 2, h-k). Assuming that at least $H_2PC2^{\bullet-}$ and $H_2PC3^{\bullet-}$ have a very similar relaxation behavior (as they differ only in the sites of the propyl substituents), this infers that for $H_2PC3^{\bullet-}$ more protons than just the two (N-H) protons have to be assigned to a_1. Furthermore, the Special TRIPLE spectrum of $H_2PC3^{\bullet-}$ suggests that four equivalent protons contribute to the largest positive hfc, a_7, because line 2 in Figure 3c, corresponding to this hfc, is close in intensity to lines 3 and 4 to each of which four protons were assigned (hfc's a_3 and a_4). We therefore assigned only four β-protons of the propyl substituents to a_7, thus assuming the eight β-protons to be no longer equivalent, which is in contrast to $H_2PC2^{\bullet-}$. The eight β-protons split into two sets of four equivalent protons, one of them corresponding to a_7, the other one either to a_1 or to a_6. As far as the two smallest hfc's, a_1 and a_6, are concerned, we are only certain that the two (N-H) protons contribute to a_1 (by analogy with $H_2PC1^{\bullet-}$ and $H_2PC2^{\bullet-}$). The remaining protons to be assigned either to a_1 or to a_6 are 4 β-protons, 8 γ-protons, and 12 δ-protons of the propyl substituents. The hfc's of some of these protons can, of course, be so small that they are not detected in the ENDOR spectrum (as is the case for the γ- and δ-protons of the propyl substituents in $H_2PC2^{\bullet-}$). In the first step for an assignment, the number of protons contributing to a_1 was extracted from the areas under the different ENDOR lines. For this purpose, the spectra of $H_2PC2^{\bullet-}$ and $H_2PC3^{\bullet-}$ were analyzed with COMPASS,[27] a computer program for the deconvolution of strongly overlapping lines. From the Special TRIPLE spectrum of $H_2PC2^{\bullet-}$ (Figure 3b) and from the absence of a_1 for $NiPC2^{\bullet-}$ and $PdPC2^{\bullet-}$, we can conclude that only the two (N-H) protons contribute to a_1 in the ENDOR spectrum of $H_2PC2^{\bullet-}$. In addition, we saw above that four protons correspond to the largest hfc, a_4, in the Special TRIPLE spectra of $H_2PC2^{\bullet-}$ and $H_2PC3^{\bullet-}$. The comparison of the ratios of the areas under the outermost ENDOR lines and the ENDOR lines corresponding to a_1 (see Figure 2, j and k) suggests that 6 to 10 protons have to be assigned to a_1 in $H_2PC3^{\bullet-}$. To further restrict the possible assignments, the ESR spectrum of $H_2PC3^{\bullet-}$ was computer-simulated with the hfc's obtained from ENDOR and assuming that the single component line width is similar to the one needed for the simulation of the ESR spectrum of $H_2PC2^{\bullet-}$. Satisfactory simulations were only obtained if 8 or 10 protons were assigned to a_1, whereas the multiplicity of a_6 was not very critical. Additional information for the assignment to molecular positions was also attempted to be gained on the basis of advanced MO calculations (see next section).

MO Calculations

The s-spin densities and total energies of the three free-base porphycenes $H_2PC1^{\bullet-}$, $H_2PC2^{\bullet-}$, and $H_2PC3^{\bullet-}$ were calculated with an all-valence-electrons SCF-MO method. This method is based on the well-known INDO approximation[28] and uses a restricted Hartree-Fock (RHF) procedure with a subsequent perturbation treatment to include spin-polarization effects in open-shell systems[7,29] (RHF-INDO/SP method). The geometry of the anion radicals was optimized by energy minimization using the simplex method for function minimization.[30]

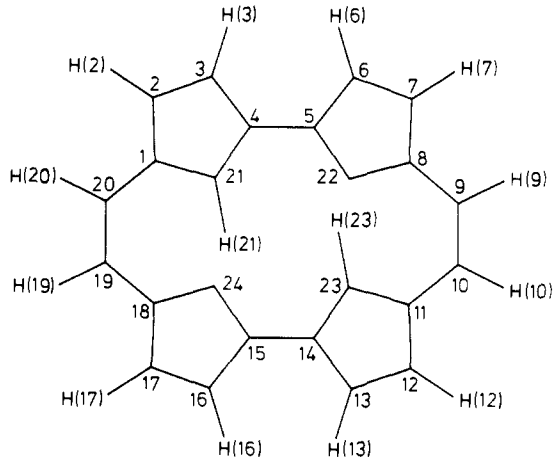

Figure 5. Energy-minimized structure and numbering scheme of $H_2PC1^{\bullet-}$.

The calculations were performed on the CRAY X-MP/24 vector computer of the Konrad-Zuse-Rechenzentrum (Berlin). An energy minimization for $H_2PC2^{\bullet-}$, for example, with 15 parameters requires a memory size of ≈250 000 words and 20 to 120 min of CPU time, depending on starting conditions and speed of convergence (the mean standard energy error being $\epsilon = 10^{-5}$ au[7]). The starting values of the various geometrical parameters were estimated from space-filling models. They were varied in a reasonable range to verify whether the simplex contracted always to the same minimum. These investigations showed that bond lengths always converged to the same values within 0.005 Å, whereas bond angles varied within 1° and dihedral angles within 2-12° (depending on the dihedral angle considered). Effects of these variations on the s-spin densities of α-protons and ^{14}N atoms are very small (≤2%). On the other hand, small variations of the dihedral angles can change the s-spin densities of β-protons (of $H_2PC2^{\bullet-}$ and $H_2PC3^{\bullet-}$) by up to a factor of 3. For $H_2PC2^{\bullet-}$ and $H_2PC3^{\bullet-}$ we therefore carefully studied how the total energy of the molecule depends on variations of the dihedral angles.

$H_2PC1^{\bullet-}$. The basic porphycene skeleton was taken to be strictly planar. The peripheral α-protons were placed in the porphycene plane. Bond lengths and angles were determined by energy minimization. With an additional parameter (the dihedral angle $\theta_{2,1,21,H(21)}$; see Figure 5), we allowed the two (N-H) protons to lie on different sides of the porphycene plane. Since the ENDOR spectra indicate that the molecule has D_{2h} symmetry (all four nitrogens are equivalent, as well as the four protons at positions 2, 7, 12, 17, the four protons at positions 3, 6, 13, 16, the four protons at positions 9, 10, 19, 20, and the two (N-H) protons), we presupposed this symmetry to construct the parametrized geometry of the molecule, with the exception that the (N-H) protons were "attached" to two diagonally opposite nitrogens, 21 and 23 (see Figure 5). By further assuming that the bond lengths $r_{1,2}$ and $r_{3,4}$ and the bond angles $\beta_{20,1,2}$ and $\beta_{3,4,5}$ are equal, 14 parameters (8 bond lengths, 5 bond angles, and 1 dihedral angle) were varied simultaneously. The bond lengths and angles resulting from energy minimization are summarized in Table II.

Figure 5 shows the energy-minimized structure of $H_2PC1^{\bullet-}$. An energy minimum was found for an in-plane position of the (N-H) protons (as indicated by X-ray data[1]). Another important result of these calculations is that for the energy-minimized structure the two (N-H) protons come to lie on the long axis of the molecule, thus forming symmetrical N—H···N bonds and leading to D_{2h} symmetry of the molecule. This point will be discussed in detail below. Furthermore, our calculations show that none of the MO's are accidentally degenerate.

The results of the spin density calculations for the energy-minimized structure are depicted in Figure 6 together with the

(26) Kirste, B. *J. Magn. Reson.* **1987**, *73*, 213.
(27) Tränkle, E.; Lendzian, F. *J. Magn. Reson.* **1989**, *84*, 537.
(28) Pople, J. A.; Beveridge, D. L. *Approximate Molecular Orbital Theory*; McGraw-Hill: New York, 1970.
(29) Plato, M.; Lubitz, W.; Lendzian, F.; Möbius, K. *Isr. J. Chem.* **1988**, *28*, 109.
(30) Nelder, J. A.; Mead, R. *Comput. J.* **1965**, *7*, 308.

Table II. Geometrical Parameters Resulting from Energy Minimization for $H_2PC1^{\bullet-}$, $H_2PC2^{\bullet-}$, and $H_2PC3^{\bullet-}$ [a]

	atom		distance (Å)		atom			bond angle (deg)	
	1	2	our MO calcns	X-ray data[1] (av)	1	2	3	our MO calcns	X-ray data[1] (av)
$H_2PC1^{\bullet-}$	1	2	1.41	1.43	1	2	3	108.0	108
	2	3	1.38	1.35	3	4	5	127.9	130
	4	5	1.42	1.40	8	9	10	129.7	132
	4	21	1.39	1.36	3	4	21	107.9	108
	21	H(21)	1.23	0.89	3	2	H(2)	127.1	129
	2	H(2)	1.12	0.99	8	9	H(9)	113.9	113
	8	9	1.42	1.40	1	21	H(21)	117.0	122
	9	10	1.36	1.39					
$H_2PC2^{\bullet-}$	4	5	1.42		1	2	3	107.3	
	8	9	1.42		3	4	5	127.3	
	9	10	1.36		8	9	10	129.9	
	4	21	1.38		3	4	21	108.9	
	21	H(21)	1.22		2	3	H(3)	126.8	
	2	2^1	1.47		8	9	H(9)	114.3	
	2^1	2^2	1.48		1	21	H(21)	117.2	
					3	2	2^1	126.4	
$H_2PC3^{\bullet-}$	1	2	1.42		1	2	3	108.0	
	8	9	1.43		3	4	5	127.2	
	9	10	1.39		8	9	10	128.3	
	4	21	1.39		3	4	21	107.5	
	21	H(21)	1.22		3	2	H(2)	125.9	
	9	9^1	1.48		1	21	H(21)	117.6	
	9^1	9^2	1.48		8	9	9^1	113.3	
	9^1	H(9^1)	1.13						

[a] For $H_2PC1^{\bullet-}$ X-ray data[1] are shown for comparison.

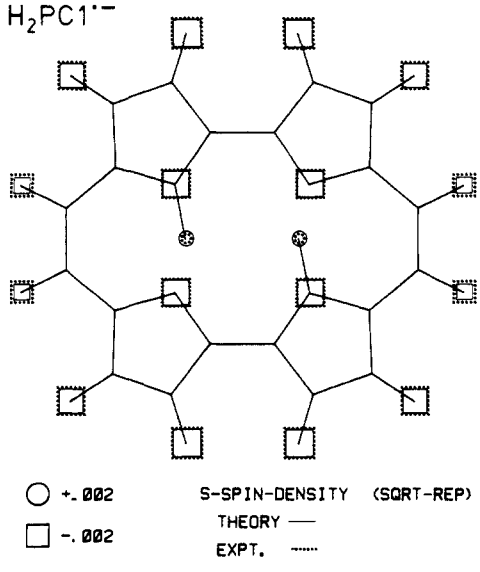

Figure 6. Comparison of experimental (dotted lines) and calculated (solid lines) s-spin densities for $H_2PC1^{\bullet-}$. Their values are proportional to the area of the squares ($\rho < 0$) and circles ($\rho > 0$). Experimental values are from isotropic hfc's using $Q(^1H) = 1420$ MHz and $Q(^{14}N) = 650$ MHz (29).

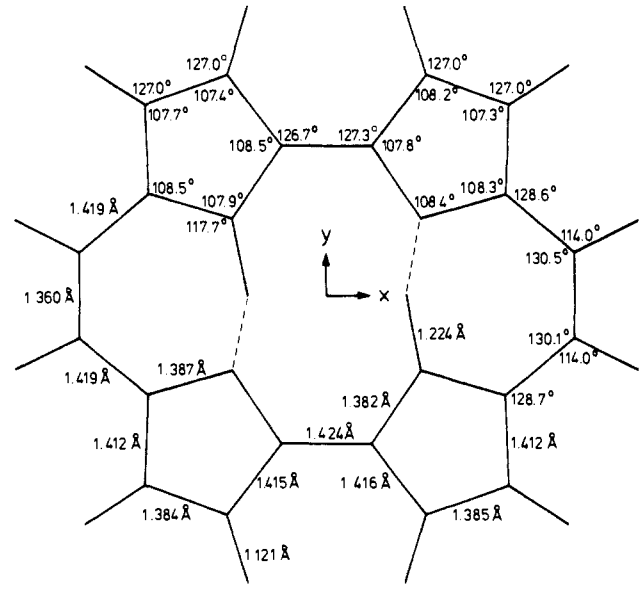

Figure 7. Energy-minimized structure of $H_2PC1^{\bullet-}$ when 13 bond lengths and 19 bond angles are varied simultaneously. The numerical error is approximately ±0.005 Å for bond lengths and ±1° for bond angles.

experimental results (see also Table III). The agreement between theory and experiment is quite satisfactory and confirms the assignment given in the preceding section. Furthermore, we can now assign the hfc's a_3 and a_4 to the two sets of equivalent α-protons at positions 2, 7, 12, 17 and 3, 6, 13, 16, respectively.

The position of the (N-H) protons requires further discussion. The result of the MO calculations concerning the symmetrical N—H···N bonds implies that this D_{2h} symmetry of the molecule is energetically favored as compared with C_{2h} symmetry, although the N-H bond length now is as large as 1.23 Å (for comparison, the standard N-H bond length is 1.01 Å). The question arises as to whether the result for the energy-minimized geometry of $H_2PC1^{\bullet-}$ is a consequence of our assumption that the structures of the four pyrrole rings are equivalent. By this we enforced an approximate D_{2h} symmetry upon the molecule to start with which may not be justified. To elucidate this problem we did further MO calculations starting from a structure with C_{2h} symmetry. Within the limits of C_{2h} symmetry, but with the further restriction that all C-H bonds are equal ($r_{C-H} = 1.12$ Å as taken from our energy minimization with 14 parameters; see Table II), all bond lengths and angles, 32 parameters in total, were varied simultaneously. The resulting energy-minimized structure is shown in Figure 7. The deviations from the previously optimized structure depicted in Figure 5 are very small; bond lengths coincide within 0.005 Å and bond angles within 1.2°. Again, the (N-H) protons come to lie exactly in-between two adjacent nitrogens (21 and 24, 22 and 23, respectively) leading to D_{2h} molecular symmetry within the numerical error of the algorithm used. We further performed MO calculations on the neutral H_2PC1 molecule (again with 32 parameters) and on the anion radical with changed bonding parameters (β_A^0 in the INDO approximation[31]) for the nitrogen atoms (22 or 28 eV instead of the standard value of 25 eV). In all cases the energy-minimized structure had D_{2h} sym-

(31) Pople, J. A.; Beveridge, D. L. In ref 28, p 72.

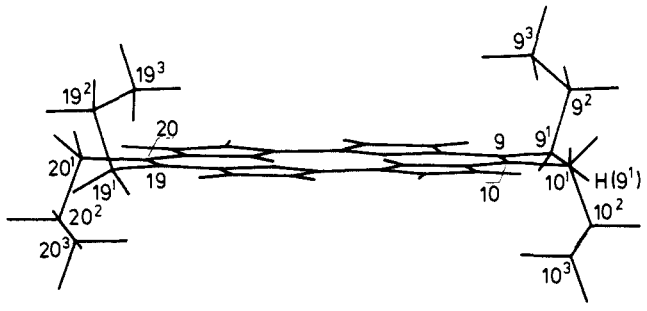

Figure 8. Energy-minimized structure and numbering scheme of $H_2PC3^{\bullet-}$ (bent conformation, perspective view).

metry. A comparison of the optimized geometries of the neutral molecule and the anion radical indicates that the conformations of these two species are very similar. Bond lengths coincide within 0.02 Å and bond angles within 0.2°. This is in agreement with recent EXAFS studies on $NiPC2^{\bullet-}$.[6c] Furthermore, the energy-minimized structure of $H_2PC1^{\bullet-}$, and thus also of H_2PC1, is very similar to the structure determined from X-ray data[1] (see Table II). The small discrepancies might either be due to shortcomings of the MO theory or, more probably, to effects of crystal forces exerted on the molecule in the solid-state.

Additional MO calculations were done to investigate the potential energy surface when the position of the (N-H) protons was varied in the vicinity of the energy minimum. The molecule was taken to be planar and, for a given position of the (N-H) protons, the whole rest of the molecule was allowed to relax in the plane. These calculations required an energy minimization with 30 parameters. The resulting total energy surface turned out to have a single minimum. Its analytical form is given by

$$E_{pot} = a + b(x - 1.26)^2 + cy^2 + d(x - 1.26)^3$$

where x and y refer to axes shown in Figure 7, and a equals E_{pot} in the energy minimum. If x and y are given in Å and E_{pot} in eV, $b = 8.0$ eV·Å^{-2}, $c = 12.1$ eV·Å^{-2}, and $d = 32.0$ eV·Å^{-3}. This represents a shallow minimum in which a displacement by 0.03 Å, for example, results in $\Delta E = 0.03$ eV ($\cong 1$ kT at room temperature). This appears to be in contradiction with ^{15}N-CPMAS-NMR experiments[15] on porphycenes that show fast N-H tautomerization in conjunction with strong, asymmetrical N—H···N hydrogen bonds. Consequently, according to NMR spectroscopy, the (N-H) protons move along a double minimum potential path whose potential barrier, however, is very low ($\cong 7 \times 10^{-3}$ eV $\triangleq$ 0.28 kT at room temperature[15]). This is different from the situation for free-base porphyrins where the potential barrier is significantly higher ($\cong$0.4 eV[15]), thus leading to slower (N-H) tautomerization. When comparing NMR and ESR results it should be kept in mind, however, that ^{15}N-CPMAS-NMR experiments were performed with neutral species in crystalline form and not with anion radicals in solution as in the ESR/ENDOR experiments.

In solution, we have to consider two possibilities: (i) a static situation with symmetrical N—H···N bonds or (ii) a dynamic situation with a fast jump process of the (N-H) protons leading to D_{2h} symmetry on the time average of the ESR/ENDOR experiments. Since we are dealing with very shallow potential minima in both cases, MO theory alone is not reliable enough to distinguish between these two possibilities. Compatible with the assumption of symmetrical N—H···N hydrogen bonds are the IR spectra of porphycenes; as opposed to porphyrins, no NH stretching bands have been observed in the range between 3300 and 3360 cm^{-1}. This is in favor of long NH bonds and strong N—H···N hydrogen bonds.[1]

$H_2PC3^{\bullet-}$. As for $H_2PC1^{\bullet-}$, the basic porphycene skeleton was taken to be planar. All α-protons as well as the β-C atoms[32] and the two (N-H) protons were placed in the porphycene plane. Nine bond lengths were varied. For $r_{2,3}$, $r_{2,H(2)}$, and $r_{4,5}$ (see Figure 5),

(32) β-C atoms are one bond away from the π-system.

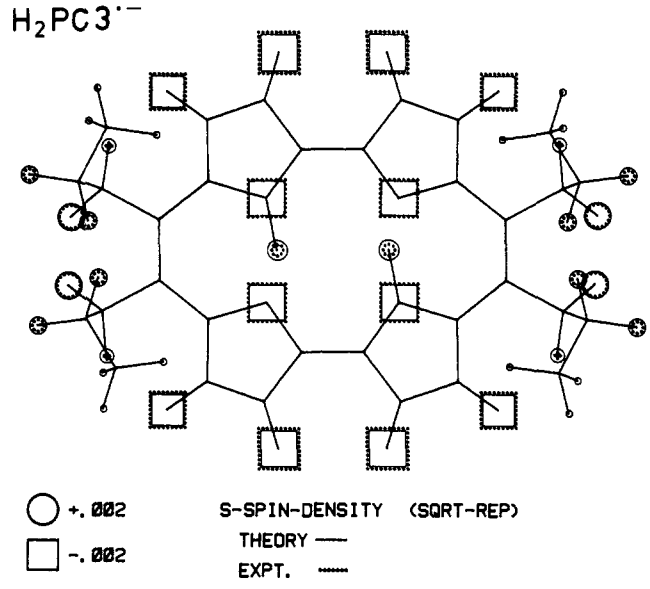

Figure 9. Comparison of experimental (dotted lines) and calculated (solid lines) s-spin densities for $H_2PC3^{\bullet-}$. For details, see caption of Figure 6. An average value was taken for the theoretical s-spin densities of the δ-protons.

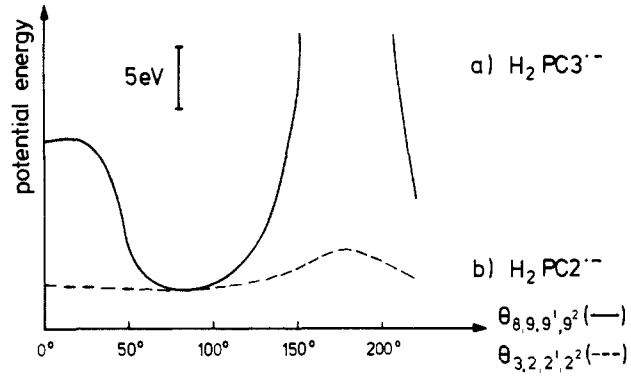

Figure 10. (a) Total energy of the $H_2PC3^{\bullet-}$ molecule as a function of the dihedral angle $\theta_{8,9,9^1,9^2}$ (solid line). (b) Total energy of the $H_2PC2^{\bullet-}$ molecule as a function of the dihedral angle $\theta_{3,2,2^1,2^2}$ (dotted line). The potential curves are symmetrical with respect to $\theta = 180°$.

values of the energy-minimized structure of $H_2PC1^{\bullet-}$ were taken. All C-H bonds of the propyl substituents were assumed to have equal length. The same five bond angles as for $H_2PC1^{\bullet-}$ were varied. For the C-C-C and C-C-H bond angles of the propyl substituents, the standard tetrahedral angle of 109.47° was used. Two further parameters were the dihedral angles $\theta_{8,9,9^1,9^2}$ and $\theta_{9,9^1,9^2,9^3}$ (see Figure 8). The bond lengths and angles resulting from energy minimization are collected in Table II. An energy minimum was found for $\theta_{8,9,9^1,9^2} = 93°$ and $\theta_{9,9^1,9^2,9^3} = -80°$. This corresponds to a conformation that we will name "bent" because the propyl substituents are bent toward the porphycene skeleton. A perspective view of the energy-minimized structure of $H_2PC3^{\bullet-}$ is shown in Figure 8. The result of the spin density calculations for the energy-minimized structure is depicted in Figure 9 together with the experimental results. Again, the agreement between theory and experiment is quite satisfactory. Another local minimum was found for $\theta_{8,9,9^1,9^2} = 89°$ and $\theta_{9,9^1,9^2,9^3} = 172°$. This corresponds to the "stretched" conformation where the propyl substituents point away from the porphycene skeleton. The potential energy of the "stretched" conformation is only $\cong$0.03 eV above that of the "bent" conformation.

For both conformations the calculations show the inequivalence of the β-protons leading to two different β-proton hfc's (corresponding to ρ_{β_1} and ρ_{β_2} in Table III). Since inequivalent β-proton hfc's can be due to hindered rotation of the propyl chains, we studied how the total energy of the molecule changes as a function of the dihedral angle $\theta_{8,9,9^1,9^2}$. The result is shown in Figure 10a.

Table III. Theoretical and Experimental ^1H and ^{14}N s-Spin Densities of $H_2PC1^{\bullet-}$, $H_2PC2^{\bullet-}$, and $H_2PC3^{\bullet-}$

		$H_2PC1^{\bullet-}$		$H_2PC2^{\bullet-}$		$H_2PC3^{\bullet-}$			
		exptl	calcd	exptl	calcd	exptl	stretched calcd	bent calcd	assignment
H:	ρ_1[a]	+0.000 36	+0.000 89	+0.000 34	+0.000 85	+0.000 30	+0.000 87	+0.000 86	(N–H) protons
	ρ_2	−0.001 89	−0.001 02	−0.001 78	−0.001 02				α-protons at positions 9, 10, 19, 20
	ρ_3	−0.002 89	−0.002 27			−0.002 69	−0.002 09	−0.002 12	α-protons at positions 2, 7, 12, 17
	ρ_4	−0.003 54	−0.002 94	−0.003 11	−0.002 58	−0.003 52	−0.002 88	−0.002 76	α-protons at positions 3, 6, 13, 16
	ρ_5			+0.002 08	+0.001 80				β-protons at positions 2^1, 7^1, 12^1, 17^1
	ρ_6					+0.000 07[b]			
	ρ_7					+0.001 18			
							+0.000 58[c]	+0.000 41	ρ_{β_1} β-protons at positions 9^1, 10^1, 19^1, 20^1
							+0.001 26	+0.001 55	ρ_{β_2}
							+0.000 09	+0.000 11	ρ_{γ_1} γ-protons at positions 9^2, 10^2, 19^2, 20^2
							−0.000 12	+0.001 16	ρ_{γ_2}
							+0.000 08	−0.000 09	ρ_δ δ-protons at positions 9^3, 10^3, 19^3, 20^3
N:	ρ_N	−0.003 08	−0.002 63	−0.003 05	−0.002 51	−0.003 00	−0.002 62	−0.002 61	nitrogens

[a] The experimental s-spin densities ρ_i (i = 1, ..., 7, N) correspond to the isotropic hfc's a_i, converted with $Q(^1H)$ = 1420 MHz and $Q(^{14}N)$ = 650 MHz (29). [b] For $H_2PC3^{\bullet-}$ ρ_6 and ρ_7 could not definitely be assigned. [c] Two s-spin densities are given both for the β- and for the γ-protons corresponding to two sets of four equivalent protons. An average value was taken for the theoretical s-spin densities of the δ-protons.

The molecule was locked to the energy-minimized structure except for the dihedral angle $\theta_{9,9^1,9^2,9^3}$ which was optimized for each given $\theta_{8,9,9^1,9^2}$ so that the end of the propyl chain could relax to the position with lowest total energy of the molecule. The energy curve around the minimum at $\theta_{8,9,9^1,9^2}$ = 93° is very steep; the energy barrier between 0° and 90°, for example, is ≅11 eV. We conclude that, because of steric hindrance, the β-protons of the propyl substituents are locked and give rise to two different β-proton hfc's. This is confirmed in the experiment where only four β-protons could be assigned to a_7 (see previous section). Furthermore, the calculations show that for the stretched conformation γ- and δ-protons have very small s-spin densities (see Table III) as they are more remote from the π-system of the porphycene skeleton. For this conformation we would have to assign four β-protons together with the two (N–H) protons to a_1 (see footnote *a* in Table III) while an unknown number of γ- and/or δ-protons contributes to a_6, the remaining assignment being as already described in the previous section. For the bent conformation, on the other hand, only four of the γ-protons and the δ-protons (see ρ_{γ_1} and ρ_δ in Table III) have very small s-spin densities, whereas the other four equivalent γ-protons have an s-spin density, ρ_{γ_2}, that is larger than ρ_7. If the ends of the propyl substituents are twisted slightly out of their energy-minimized position, ρ_{γ_2} decreases while ρ_{γ_1} increases. Thus, two cases have to be considered. In the first case, we assume that the γ-protons merely oscillate around their equilibrium position and, consequently, are inequivalent so that only four γ-protons are assigned to a_1 together with the two (N–H) protons. The four β-protons of the substituents that have not yet been assigned can then be attributed either to a_1 or to a_6 and the other four γ-protons together with an unknown number of δ-protons to a_6. In the second case, we assume that the γ-protons rotate freely, giving eight equivalent γ-protons with an s-spin density of ≅0.000 80 (a ≅ 1.1 MHz). In this case eight γ-protons together with the two (N–H) protons could be assigned to a_1, whereas the four β-protons would contribute to a_6. Whether the δ-protons contribute to a_6 as well cannot be decided. We tend to favor this last assignment, with the bent conformation and freely rotating γ-protons, since it is the one with the best overall agreement between experiment, ESR simulations, COMPASS analysis, and MO calculations. But none of the methods is powerful enough to definitely exclude any of the other assignments discussed.[33]

$H_2PC2^{\bullet-}$. As for $H_2PC1^{\bullet-}$, the basic porphycene skeleton was taken to be planar. All α-protons, as well as the β-C atoms and the two (N–H) protons, were situated in the porphycene plane. Seven bond lengths were varied. For $r_{1,2}$, $r_{2,3}$, $r_{3,H(3)}$, and $r_{2^1,H(2^1)}$ (see Figure 11), values from the energy-minimized structure of $H_2PC1^{\bullet-}$ and $H_2PC3^{\bullet-}$ were taken. All C–H bond lengths of the propyl substituents were again assumed to be equal. The six bond angles varied were the same as for $H_2PC1^{\bullet-}$ with the addition of $\beta_{3,2,2^1}$. For all C–C–C and C–C–H bond angles of the propyl substituents, the standard tetrahedral angle of 109.47° was used. The dihedral angles $\theta_{3,2,2^1,2^2}$ and $\theta_{2,2^1,2^2,2^3}$ were two additional variable parameters. The bond lengths and angles are summarized in Table II. A shallow energy minimum was found for $\theta_{3,2,2^1,2^2}$

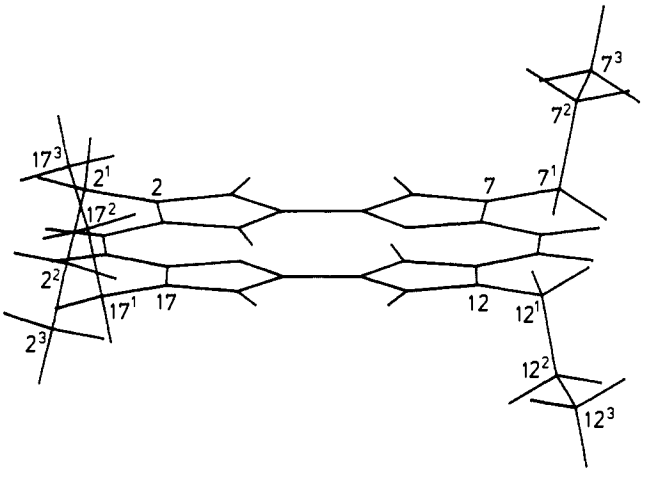

Figure 11. Energy-minimized structure of $H_2PC2^{\bullet-}$, perspective view.

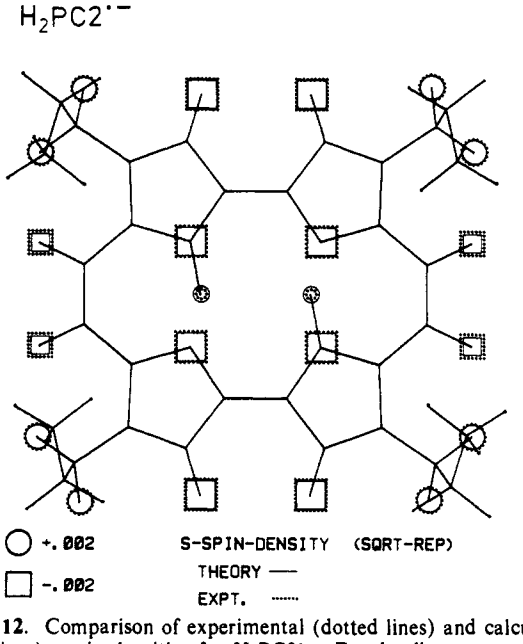

Figure 12. Comparison of experimental (dotted lines) and calculated (solid lines) s-spin densities for $H_2PC2^{\bullet-}$. For details, see caption of Figure 6. For the β-, the γ-, and the δ-protons the s-spin densities were averaged.

(33) The suggestion by a referee that the relative complexity of the ESR and ENDOR spectra of $H_2PC3^{\bullet-}$ might be due to the presence of reduction products, such as a pyrrolophane,[1b] has been followed up but could not be substantiated.

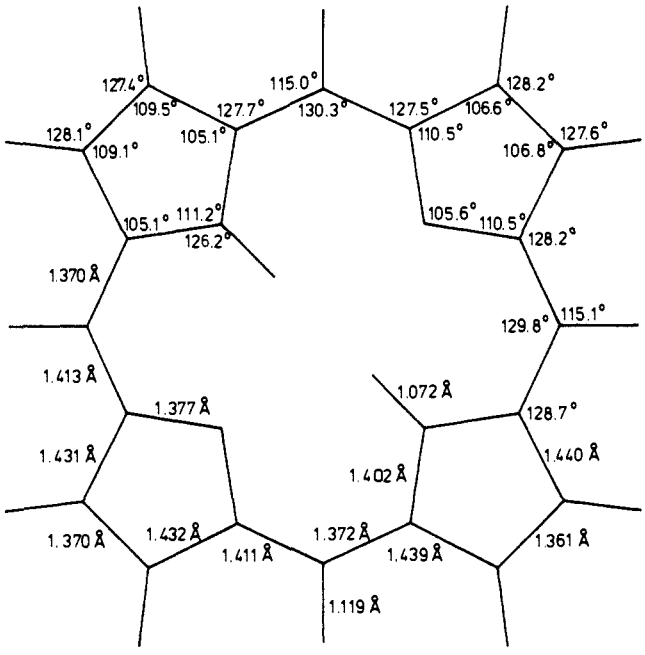

Figure 13. Energy-minimized structure of free-base porphyrin, 14 bond lengths and 17 bond angles were varied simultaneously. The numerical error is approximately ±0.005 Å for bond lengths and ±1° for bond angles.

= 81° and $\theta_{2,2^1,2^2,2^3} = 65°$. A perspective view of the energy-minimized structure of $H_2PC2^{\bullet-}$ is shown in Figure 11. The result of the spin density calculations for this structure is depicted in Figure 12 together with the experimental results. Here, also, theory and experiment agree quite well.

In Figure 10b the total energy of the molecule is plotted as a function of the dihedral angle $\theta_{3,2,2^1,2^2}$ (the rest of the molecule was again locked except for the dihedral angle $\theta_{2,2^1,2^2,2^3}$ and the bond angle $\beta_{3,2,2^1}$ which were optimized). As opposed to the case of $H_2PC3^{\bullet-}$ the energy curve around the minimum at $\theta_{3,2,2^1,2^2} \cong 81°$ is quite shallow. The energy barrier between 0° and 80°, for example, is ≅0.4 eV. Thus, in contrast to $H_2PC3^{\bullet-}$, where the propyl chains appear to be locked, in $H_2PC2^{\bullet-}$ the propyl chains can move more or less freely around their equilibrium positions. This explains why only one β-proton hfc is observed in the ENDOR spectrum.

Porphyrin. For comparison, a geometry optimization was also performed for the free-base porphyrin anion. As for $H_2PC1^{\bullet-}$, we supposed that the molecule is planar and started from a porphyrin geometry with C_{2h} symmetry, the only restriction being again that all C–H bonds were equal. As many as 14 bond lengths and 17 bond angles were varied simultaneously. The resulting energy-minimized structure is depicted in Figure 13. The (N–H) protons are localized at two diagonally opposite nitrogen atoms, the N–H bond length being 1.07 Å. Furthermore, the diagonally opposite pyrrole rings are pairwise equivalent within the numerical error of the algorithm used with the consequence that the porphyrin skeleton has static D_{2h} symmetry. This is in agreement with earlier X-ray measurements[34] and MO calculations[35] on neutral porphyrins.[36] Thus, in the case of porphyrin, we find that each (N–H) proton is bound to one nitrogen, whereas in the case of porphycene, according to the MO calculations, each (N–H) proton is symmetrically bound to two nitrogens, the N–H bond length being very long (r_{N-H} = 1.23 Å).

Conclusion

Detailed information on the electronic and geometrical structures of several porphycene anion radicals was obtained from ESR, ENDOR, and TRIPLE resonance experiments in conjunction with MO calculations. The results are of particular interest in comparison to known structural characteristics of the isomeric porphyrins which frequently serve as electron donors in electron transfer systems modeling photosynthetic charge separation.

The most prominent difference in the spectroscopic behavior of porphyrin and porphycene radical anions results from an orbital degeneracy (or near degeneracy) in the porphyrins leading to unresolved hfs, whereas this is not the case in porphycenes which show ESR spectra with resolved hfs. Another important difference between free-base porphyrin and free-base porphycene anions evident from this study (and for the neutral molecules from independent NMR experiments) exists in the bonding behavior of the (N–H) protons. In contrast to the porphyrin anions, the (N–H) protons in the porphycene anions undergo a fast N—H↔N tautomerization process (dynamic model) or are characterized by the formation of symmetrical N–H–N bonds (static model). Both models lead to (apparent) D_{2h} symmetry of the porphycenes.

Furthermore, the results of this study are of interest with regard to on-going experiments on light-induced charge separation. In these experiments the following question is raised: How do the electronic and structural differences between porphyrin and porphycene donors affect the electron transfer rates to the quinone acceptors? To answer this question, detailed knowledge of the LUMO of the isomeric donor molecules would be helpful since it is the LUMO of the donor which participates in the photoinitiated electron transfer via an excited singlet- or triplet-state precursor. This LUMO can be modeled by the half-filled orbital of the porphyrinoid anion radicals.

To learn more about the electronic structure of the isomers, a different approach would be the comparison of the *cation* radicals of porphyrins and porphycenes. With respect to the porphyrins, this would have the advantage that at least in one class of porphyrin cation radicals (those with a ground state of A_{2u} symmetry) the ESR spectra are well resolved[37,38] and, using ENDOR, the hfc's of several porphyrins of that class were determined.[39-41] Even though this is not the case for the other class of porphyrin cation radicals (the ESR spectra of these radicals with A_{1u} ground state are only partially resolved[37,38]), a comparison of the cation radicals of porphyrins and porphycenes would certainly be an interesting issue for further studies.

Acknowledgment. We thank Drs. Friedhelm Lendzian (Free University of Berlin) for clarifying discussions concerning the multiplicity of the hfc's for $H_2PC3^{\bullet-}$, Georg Hohlneicher (University of Cologne) for helpful discussions about the position of the (N–H) protons, and Jack Fajer (Brookhaven National Laboratory) for preprints of his work on nickel porphycene (ref 6b,c). We appreciate the constructive criticism of the referees. This work was supported by the Deutsche Forschungsgemeinschaft (FUB, HUJ) and by the Israel Council for Research and Development (HUJ). The Fritz Haber Research Center is supported by the Minerva Gesellschaft für die Forschung GmbH, München, FRG.

(34) Webb, L. E.; Fleischer, E. B. *J. Chem. Phys.* **1965**, *43*, 3100. Chen, B. M. L.; Tulinsky, A. *J. Am. Chem. Soc.* **1972**, *94*, 4144. Tulinsky, A. *Ann. N.Y. Acad. Sci.* **1973**, *206*, 47.

(35) Almlöf, J. *Int. J. Quantum Chem.* **1974**, *8*, 915. Sarai, A. *J. Chem. Phys.* **1982**, *76*, 5554; **1984**, *80*, 5341. Kuzmitsky, V. A.; Solovyov, K. N. *J. Mol. Struct.* **1980**, *65*, 219. Bersuker, G. I.; Polinger, V. Z. *Chem. Phys.* **1984**, *86*, 57.

(36) Neutral porphyrins and their anion radicals are assumed to have the same symmetry. See, for example, ref 37.

(37) Fajer, J.; Borg, D. C.; Forman, A.; Dolphin, D.; Felton, R. H. *J. Am. Chem. Soc.* **1970**, *92*, 3451.

(38) Fajer, J.; Davis, M. S. In *The Porphyrins*; Dolphin, D., Ed.; Academic Press: New York, 1979; Vol. 4, p 197. Hanson, L. K.; Chang, C. K.; Davis, M. S.; Fajer, J. *J. Am. Chem. Soc.* **1981**, *103*, 663.

(39) Huber, M., Ph.D. Thesis, Free University of Berlin, West Germany, 1989, and references therein.

(40) Huber, M.; Galili, T.; Möbius, K.; Levanon, H. *Isr. J. Chem.* **1989**, *29*, 65.

(41) Huber, M.; Kurreck, H.; v. Maltzan, B.; Plato, M.; Möbius, K. *J. Chem. Soc., Faraday Trans.* **1990**, *86*, 1087.